Moesin Interacts with the Cytoplasmic Region of Intercellular Adhesion Molecule-3 and Is Redistributed to the Uropod of T Lymphocytes during Cell Polarization

Juan M. Serrador,* José L. Alonso-Lebrero,* Miguel A. del Pozo,* Heinz Furthmayr,‡ Reinhard Schwartz-Albiez,§ Javier Calvo,‖ Francisco Lozano,‖ and Francisco Sánchez-Madrid*

Servicio de Inmunología, Hospital de la Princesa, Universidad Autónoma de Madrid, 28006 Madrid, Spain;‡Department of Pathology, Stanford University, Stanford, California 94305-5324;§Tumor Immunology Program, German Cancer Research Center, Heidelberg, Germany D-69120; and ‖Servei Inmunología, Hospital Clinic, 08036 Barcelona, Spain

Abstract. During activation, T lymphocytes become motile cells, switching from a spherical to a polarized shape. Chemokines and other chemotactic cytokines induce lymphocyte polarization with the formation of a uropod in the rear pole, where the adhesion receptors intercellular adhesion molecule-1 (ICAM-1), ICAM-3, and CD44 redistribute. We have investigated membrane–cytoskeleton interactions that play a key role in the redistribution of adhesion receptors to the uropod. Immunofluorescence analysis showed that the ERM proteins radixin and moesin localized to the uropod of human T lymphoblasts treated with the chemokine RANTES (regulated on activation, normal T cell expressed, and secreted), a polarization-inducing agent; radixin colocalized with arrays of myosin II at the neck of the uropods, whereas moesin decorated the most distal part of the uropod and colocalized with ICAM-1, ICAM-3, and CD44 molecules. Two other cytoskeletal proteins, β-actin and α-tubulin, clustered at the cell leading edge and uropod, respectively, of polarized lymphocytes. Biochemical analysis showed that moesin coimmunoprecipitates with ICAM-3 in T lymphoblasts stimulated with either RANTES or the polarization-inducing anti–ICAM-3 HP2/19 mAb, as well as in the constitutively polarized T cell line HSB-2. In addition, moesin is associated with CD44, but not with ICAM-1, in polarized T lymphocytes. A correlation between the degree of moesin–ICAM-3 interaction and cell polarization was found as determined by immunofluorescence and immunoprecipitation analysis done in parallel. The moesin–ICAM-3 interaction was specifically mediated by the cytoplasmic domain of ICAM-3 as revealed by precipitation of moesin with a GST fusion protein containing the ICAM-3 cytoplasmic tail from metabolically labeled Jurkat T cell lysates. The interaction of moesin with ICAM-3 was greatly diminished when RANTES-stimulated T lymphoblasts were pretreated with the myosin-disrupting drug butanedione monoxime, which prevents lymphocyte polarization. Altogether, these data indicate that moesin interacts with ICAM-3 and CD44 adhesion molecules in uropods of polarized T cells; these data also suggest that these interactions participate in the formation of links between membrane receptors and the cytoskeleton, thereby regulating morphological changes during cell locomotion.

Activated T lymphocytes are motile cells with a high degree of asymmetry. They can emigrate to inflammatory sites in response to chemoattractant gradients and are able to interact with antigen-presenting and target cells (Crabtree and Clipstone, 1994). Different aspects of cell polarization, such as modification of plasma membrane, cytoskeletal redistribution, and polarized secretion of cytokines, have been described in T cells during cell–cell interactions (Kupfer et al., 1986, 1991; Kupfer et al., 1994). Motile T cells exhibit an inherent polarity before contact with other cells, showing a zone of high sensitivity to antigen and chemokines at the leading edge (Negulescu et al., 1996; Nieto et al., 1997), and the formation of a membrane protrusion, termed uropod, at the opposite pole of cell locomotion. It has recently been observed that the lymphocyte uropod extends from the area of adhesion towards the outer milieu, and that several adhesion mole-

Address all correspondence to F. Sánchez-Madrid, Servicio de Inmunología, Hospital de la Princesa, universidad Autónoma de Madrid, 28006 Madrid, Spain. Tel.: 34-1-4023347. Fax: 34-1-3092496. E-mail: fsmadrid/princesa@hup.es

cules (intercellular adhesion molecules [ICAMs],[1] CD44 hyaluronic receptor, and CD43) cluster in this structure (del Pozo et al., 1995). Lymphocyte polarization with uropod formation is induced by several chemokines (del Pozo et al., 1995) and other chemotactic cytokines such as interleukin-2 (IL-2) and IL-15 (Wilkinson and Liew, 1995; Nieto et al., 1996), as well as by some specific polarization-inducing ICAM-3 and CD43 mAb (Campanero et al., 1994; Sánchez-Mateos et al., 1995). In this regard, it has recently been found that the chemokine-induced redistribution of adhesion receptors ICAM-1 and -3 to the uropod plays an important role in the recruitment of other lymphocytes to inflammatory foci (del Pozo et al., 1997).

Membrane interactions with the cytoskeleton appear to be necessary in general for the formation of specialized protrusions. Since very few integral membrane proteins have been found to interact directly with actin, it is likely that accessory proteins serve to connect the actin cytoskeleton with the plasma membrane (Hitt and Luna, 1994). Possible candidates for this role are the closely related ezrin, radixin, and moesin proteins (ERM) (Tsukita et al., 1992, 1997; Bretscher, 1993; Arpin et al., 1994). Thus, previous studies have demonstrated that CD43 in thymocytes and CD44 in fibroblasts are associated with one or more of these proteins (Yonemura et al., 1993; Tsukita et al., 1994). The CD44 interaction is regulated by the small G protein Rho and phosphoinositides (Hirao et al., 1996). Ezrin, radixin, and moesin are variably associated with cell surface protrusions, such as microvilli, filopodia, microspikes, adhesion contacts, and membrane ruffling (Sato et al., 1992; Amieva and Furthmayr, 1995). Ezrin has been detected mainly in microvilli of brush border epithelial cells, such as intestinal or placental microvilli (Berryman et al., 1995; Fath and Burgess, 1995), whereas radixin is localized in adherens junctions of epithelial cells (Tsukita et al., 1989). The third member of this small protein family, membrane-organizing extension spike protein (moesin), is a 78-kD protein characterized initially as a heparin-binding protein (Lankes et al., 1988; Lankes and Furthmayr, 1991). Moesin is strongly expressed in lymphoid, endothelial, and several malignant cells types. It is colocalized with actin in microextensions but not in stress fibers (Amieva and Furthmayr, 1995; Schwartz-Albiez et al., 1995). In thymoma cells, moesin is concentrated at the tip of microvilli, and moesin antisense oligonucleotides decrease the number and length of microvilli in these cells (Takeuchi et al., 1994). Moesin has also been described as a receptor for measles and rabies viruses (Dunster et al., 1994; Sagara et al., 1995).

We have investigated the cellular localization of ERM proteins in polarized migrating lymphocytes. We have found that moesin is redistributed to the distal portion of uropods, where it is colocalized with ICAM-1, -3, and CD44. Moreover, an interaction of moesin with ICAM-3 and CD44 in T lymphocytes was demonstrated by immunoprecipitation and Western blot analysis. The moesin–ICAM-3 association was found to be mediated through the intracellular region of ICAM-3, and it correlated with the degree of cell polarity. These data suggest that moesin is important for the redistribution of adhesion molecules to the cellular uropod.

1. *Abbreviations used in this paper*: ERM, ezrin, radixin, and moesin; FN80, 80-kD fibronectin fragment; ICAM, intercellular adhesion molecule; IL, interleukin; MCP-1, monocyte chemotactic protein; RANTES, regulated on activation, normal T cell expressed, and secreted.

Materials and Methods

Antibodies, Chemokines, and Reagents

The anti–ICAM-3 HP2/19 and TP1/25, anti–VLA-4 HP2/1, anti-CD44 HP2/9, and anti-moesin/radixin 38/37 mAbs have been described (Campanero et al., 1991, 1993; Pulido et al., 1991; Lankes et al., 1988). The anti–ICAM-1 Hu5/3 mAb was kindly provided by Dr. F.W. Luscinskas (Harvard Medical School, Boston, MA). The moesin-specific polyclonal antiserum (pAb) 95/2 was raised in rabbits by immunization with recombinant human moesin and purified by affinity chromatography (Amieva and Furthmayr, 1995). The affinity-purified polyclonal antibodies 464, 457, and 454 raised against unique peptides from murine ezrin, radixin, and moesin, respectively (Winckler et al., 1994), as well as the 13/H9 mAb, which recognizes all three ERM members (Birgbauer and Solomon, 1989), were generously provided by Dr. F. Solomon (Department of Biology and Center for Cancer Research, Massachusetts Institute of Technology, Cambridge, MA). The anti–β-actin mAb, anti–α-tubulin mAb, and rabbit anti-myosin polyclonal antibodies were purchased from Sigma Chemical Co. (St. Louis, MO). P3X63 myeloma protein (IgG1, Kappa) was used as negative control. Recombinant human moesin was obtained as described (Lankes and Furthmayr, 1991). Recombinant human (rh) RANTES (regulated on activation, normal T cell expressed, and secreted) (specific activity 2–5 $\times$ 10^3 U/mg, purity >97%, endotoxin level <0.1 ng/μg cytokine) and recombinant human monocyte chemotactic protein (rhMCP-1) (purity >99%) were purchased from R&D systems (Minneapolis, MN). Butanedione monoxime was purchased from Sigma Chemical Co. The 80-kD fibronectin fragment (FN80) was a generous gift of Dr. A. García Pardo (Centro de Investigaciones Biológicas, Madrid, Spain).

Cells

Resting peripheral blood lymphocytes were isolated from fresh human blood by Ficoll Hypaque density gradient centrifugation (Pharmacia Biotech. Sverige, Uppsala, Sweden), followed by adherence incubation on plastic flasks. Human T lymphoblasts were prepared from peripheral blood mononuclear cells by treatment with phytohemagglutinin 0.5% (Pharmacia Biotech. Sverige) for 48 h. Cells were washed and cultured in RPMI 1640 (Flow Laboratories, Irvine, Scotland) containing 10% FCS (Flow Laboratories) and 50 U/ml IL-2 kindly provided by Eurocetus (Madrid, Spain). T lymphoblasts cultured by 10–15 d were used in all experiments. These cells were analyzed by flow cytometry, and their phenotype was 98% CD3, 40% CD4, 60% CD8, and 99% CD45RO. They showed a heterogeneous expression of chemokine receptors CCR2 and CCR5 (del Pozo et al., 1997; Nieto et al., 1997). The HSB-2 T lymphoblastoid cell line was kindly provided by Dr. N. Hogg (Imperial Cancer Research Fund, London, UK) and has previously been described (Dougherty et al., 1988). HSB-2 and Jurkat cell lines were grown in complete medium without the addition of IL-2.

Flow Cytometry Analysis

T lymphoblasts (2×10^6 cells/ml) were treated with RANTES at 10 ng/ml for 30 min at 37°C, fixed in 3.7% (wt/vol) paraformaldehyde in PBS, pH 7.4, and then washed at room temperature in TBS (50 mM Tris-HCl, pH 7.6, 150 mM NaCl, 0.1% NaN_3). Cell suspensions were incubated for 20 min in PBS with 80 μl mAb containing culture supernatant or pAb, followed by washing and labeling with an FITC-conjugated rabbit F(ab′)2 anti–mouse IgG (DAKOPATTS, Copenhagen, Denmark) or donkey anti–rabbit IgG (Pierce Chemical Co., Rockford, IL). For intracellular staining of ERM proteins, cells were permeabilized with 0.1% Triton X-100 for 10 min before application of the first antibody. Flow cytometry analysis was performed in a FACScan® cytofluorometer (Becton Dickinson, San José, CA), and fluorescence histograms were represented in a logarithmic scale.

Immunofluorescence Microscopy

Immunofluorescence experiments were performed as described (Del

Pozo et al., 1995). Briefly, 1×10^6 T lymphoblasts were incubated in flat-bottomed, 24-well plates (Costar Corp., Cambridge, MA) in a final volume of 400 μl complete medium on coverslips coated with FN80 at 20 μg/ml. RANTES or MCP-1 at 10 ng/ml or the polarization-inducing HP2/19 mAb at 4 μg/ml was added, and cells were allowed to remain in a cell incubator at 37°C and 5% CO_2 atmosphere. After 30 min, cells were fixed with 3.7% (wt/vol) paraformaldehyde in PBS, pH 7.4, at room temperature and then rinsed in TBS. For labeling experiments, cells were incubated with a specific mAb or pAb as follows. After washing, cells were stained with a FITC-labeled rabbit F(ab′)2 anti–mouse IgG or donkey anti–rabbit IgG (Pierce Chemical Co.). For double immunofluorescence analysis, cells treated with mAb 38/87 were saturated with 10% normal mouse serum in TBS. Then, the cells were incubated with the TP1/25 biotinylated mAb, followed by washing and labeling with (TRITC)–avidin D (Vector Laboratories, Burlingame, CA) for 30 min. In the case of cells pretreated with the mAb HP2/19, the first antibody added was the mAb anti–ICAM-3 TP1/25, whereas the second one was the biotinylated antimoesin mAb 38/87 and labeling was performed with FITC-extrAvidin (Sigma Chemical Co.) and Cy3 goat anti–mouse (Amersham Corp., Arlington Heights, FL). Cells were observed using a photomicroscope (model Lubophot-2; Nikon, Inc., Melville, NY) with 60 and 100× oil immersion objectives. The proportion of uropod-bearing cells was calculated by random choice of ten fields (60× objective) of each experiment and direct counting of total cells (400–500) and uropod-bearing cells. Preparations were photographed with Ektachrome 400 film (Eastman Kodak Co., Rochester, NY).

Immunofluorescence Digital Confocal Microscopy and Time-Lapse Video Microscopy

Samples for confocal microscopy were prepared as for conventional immunofluorescence microscopy. Codistribution of ICAM-3 and moesin was studied by performing double immunofluorescence as described above. Confocal microscopy analysis was performed using a confocal laser scanning system (model MRC-1000; Bio-Rad Laboratories Ltd., Hertfordshire, UK) and an inverted microscope (model Diaphot 200; Nikon, Inc.). Images of serial cellular sections were acquired with the Bio-Rad CoMos graphical user-interface. Time-lapse video microscopy analysis was performed as described (del Pozo et al., 1997).

Immunoprecipitation and Western Blot Analysis

Polarized T lymphoblasts adhered to FN80-coated dishes were lysed by incubation for 20 min in 1.5 ml RIPA buffer containing 0.1% SDS, 0.5% deoxycholate, 1% NP-40, 150 mM NaCl, 50 mM Tris, pH 8, 1 mM p-amidino PMSF, and 15 μg/ml leupeptin. Cell lysate was removed from the dish with a rubber policeman and then precleared by centrifugation at 10,000 *g* for 20 min. In those experiments in which cell adhesion to FN80 was not required, cells were lysed in 1.5-ml tubes. Immunoprecipitations were carried out with 45 μl of mAb directly coupled to Sepharose 4B beads (Pharmacia LKB Biotechnology) at 1 mg/ml. Proteins bound to Sepharose beads were eluted by boiling in sample buffer, subjected to 7.5% SDS-PAGE under reducing conditions, and transferred onto a nitrocellulose membrane (Millipore Corp., Bedford, MA) in Tris-glycine-methanol buffer for 25 min at 17 V using a Transfer-Blot SD Semi-Dry Transfer Cell (Bio-Rad Laboratories, Hercules, CA). To detect moesin, membranes were soaked overnight in TBS containing 3% BSA, washed three times with TBS–0.1% Tween 20 for 15 min, followed by 1 h of incubation with a 1:1,000 dilution of rabbit pAb 95/2 against moesin. After three washes, blots were incubated with a peroxidase-conjugated goat anti–rabbit IgG (Pierce Chemical Co.), and proteins were visualized using an enhanced chemiluminescence system (Amersham Corp.). Quantitative

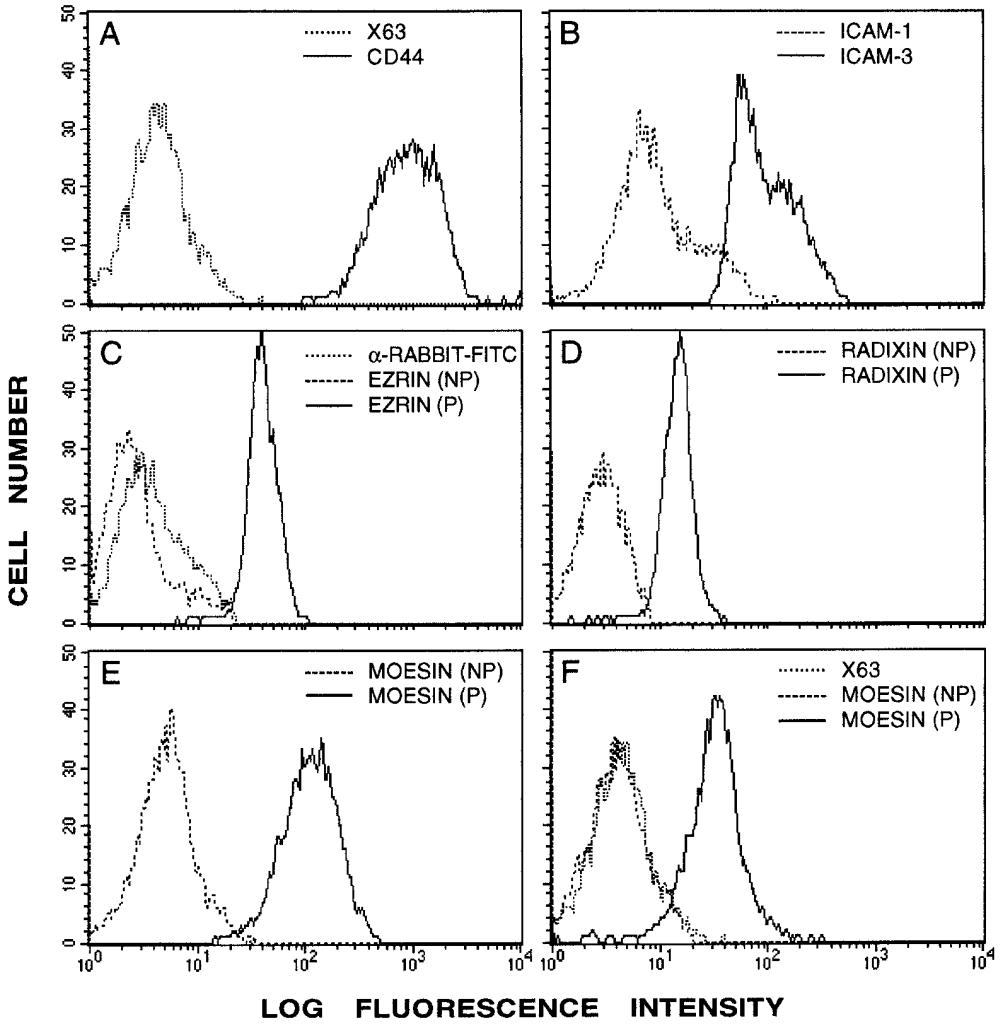

Figure 1. Flow cytometry analysis of CD44 (*A*), ICAM-1, ICAM-3 (*B*), ezrin (*C*), radixin (*D*), and moesin (*E* and *F*) in RANTES-stimulated T lymphoblasts. For the analysis of ERM expression, cells were fixed with 4% paraformaldehyde and permeabilized (*P*) or not (*NP*) with 0.1% Triton X-100 before staining with the 464 (*C*), 457 (*D*), 95/2 (*E*), and 38/37 (*F*) Abs. The staining of negative control X63 mouse myeloma protein is also shown (*dotted line*).

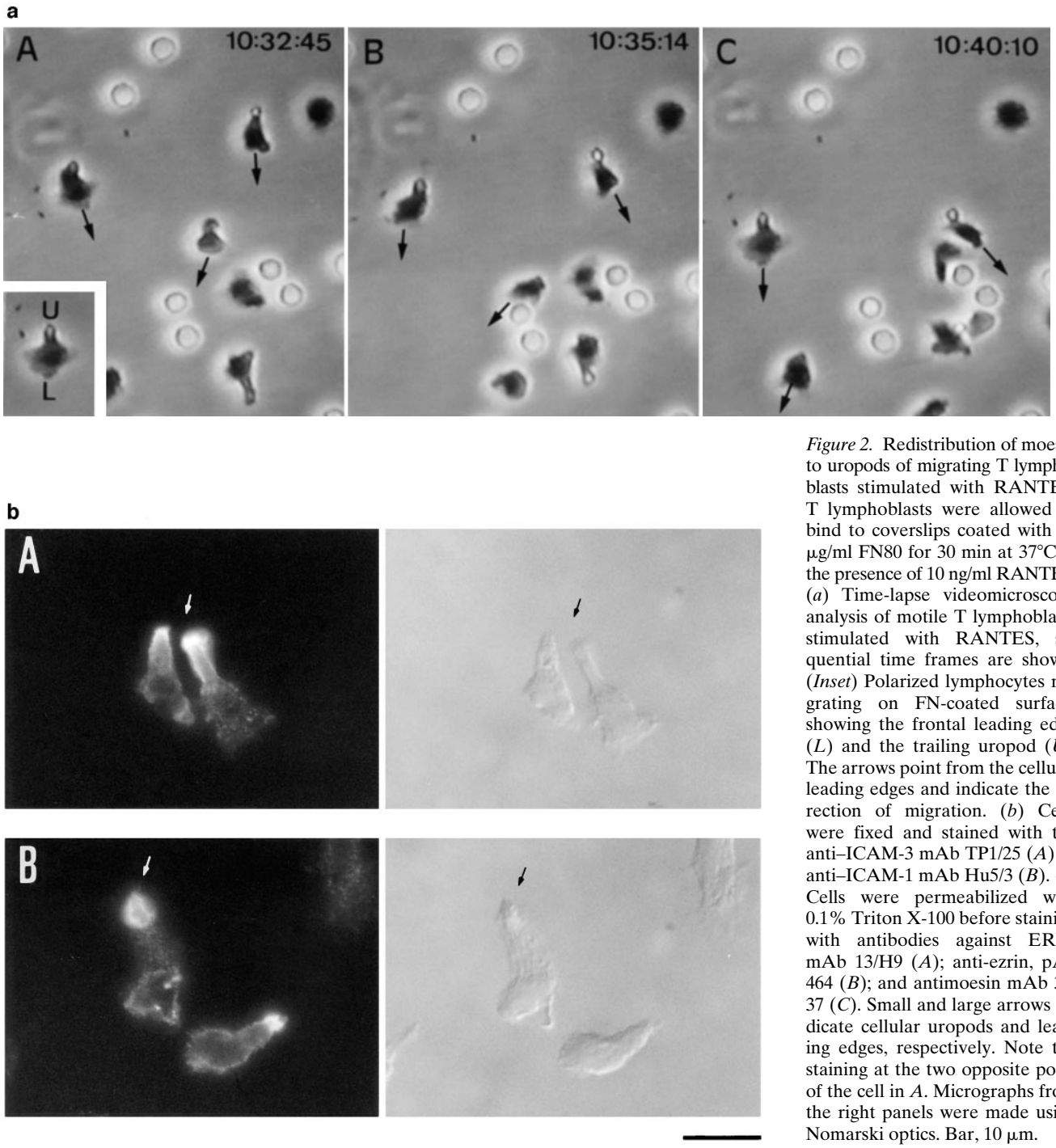

Figure 2. Redistribution of moesin to uropods of migrating T lymphoblasts stimulated with RANTES. T lymphoblasts were allowed to bind to coverslips coated with 20 μg/ml FN80 for 30 min at 37°C in the presence of 10 ng/ml RANTES. (*a*) Time-lapse videomicroscopy analysis of motile T lymphoblasts stimulated with RANTES, sequential time frames are shown. (*Inset*) Polarized lymphocytes migrating on FN-coated surface, showing the frontal leading edge (*L*) and the trailing uropod (*U*). The arrows point from the cellular leading edges and indicate the direction of migration. (*b*) Cells were fixed and stained with the anti–ICAM-3 mAb TP1/25 (*A*) or anti–ICAM-1 mAb Hu5/3 (*B*). (*c*) Cells were permeabilized with 0.1% Triton X-100 before staining with antibodies against ERM, mAb 13/H9 (*A*); anti-ezrin, pAb 464 (*B*); and antimoesin mAb 38/37 (*C*). Small and large arrows indicate cellular uropods and leading edges, respectively. Note the staining at the two opposite poles of the cell in *A*. Micrographs from the right panels were made using Nomarski optics. Bar, 10 μm.

estimation of bands were performed by densitometric analysis with NIH Image software.

Construction, Expression, and Purification of GST Fusion Proteins

The cytoplasmic regions of ICAM-3 and CD148 were amplified by PCR and cloned as SalI-NotI fragments into pGEX-4T (Pharmacia LKB Biotechnology). For amplification of the ICAM-3 cytoplasmic region (from residues R508 to E544), the primers SALCY50TH (5′-CAACGCGTCGACCAGGGAGCACCAACGG-3′) and NOTCY50TH (5′-ATAAGAATGCGGCCGCTCACTCACTCAGCTCTGGA-3′) were used. For amplification of the CD148 cytoplasmic region (from residues K999 to A1337), the primers 143CYFOR (5′-GAAGACGTCGACGAAGAGGAAAGATGCAAAG-3′) and 143CYBACK (5′-AAGATAGCGGCCGCTTAGGCGATGTAACATTGG-3′) were used.

Expression of GST fusion proteins in DH1OB cells and purification were carried out following manufacturer's instructions. The proteins were stored at 4°C on glutathione Sepharose 4B beads as a 50% slurry in 10 mM Tris, pH 7.4, 140 mM NaCl, 0.5% Triton X-l00, 0.02% azide, and protease inhibitors (Complete Protease Inhibitors; Boehringer Mannheim Corp., Indianapolis, IN). The amount of fusion proteins was estimated by Coomassie blue staining of SDS-PAGE.

In Vitro Binding of GST Fusion Proteins to Cell Extracts

Jurkat cells (2.5×10^7 cells/ml) were labeled overnight with a mixture of

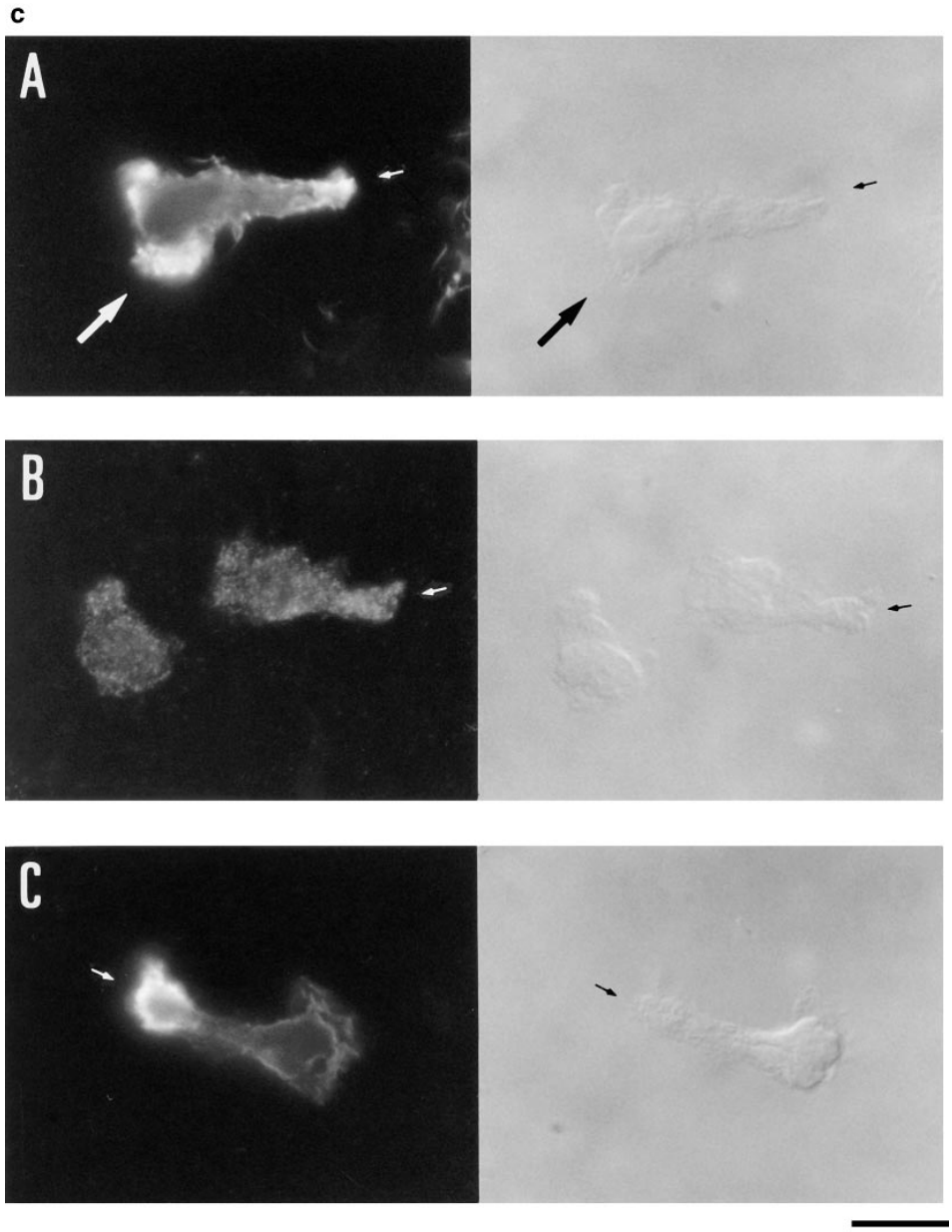

[^{35}S]methionine/cysteine (600 μCi) in methionine/cysteine-free RPMI 1640 medium supplemented with 10% dialyzed FBS. ^{35}S-labeled Jurkat cells were disrupted in 1 ml lysis buffer (10 mM Tris-HCl, pH 7.6, 150 mM NaCl, 1% NP-40, 5 mM EDTA, 50 mM sodium fluoride, 0.4 mM sodium orthovanadate, 10 mM iodoacetamide, 5 mM sodium pyrophosphate, 1 mM penoxymethyl sulphofluoride, and 10 mg/ml aprotinin, leupeptin, pepstatin A, chymostatin, and α1-antitrypsin) on ice for 10 min followed by 10 min microcentrifugation. The supernatant was mixed with ~50 μg of GST fusion proteins attached to glutathione Sepharose 4B beads for 12 h at 4°C. The beads were collected by centrifugation and washed twice with lysis buffer alone, twice with lysis buffer plus 0.1% SDS, twice with lysis buffer plus 0.65 M NaCl, and twice with lysis buffer alone. The beads were then subjected to 8% SDS-PAGE under reducing conditions.

Results

Cellular Localization of ERM Proteins in Polarized Motile T Lymphocytes

We have previously described that chemokines induce lymphocyte polarization with redistribution of several adhesion molecules, including ICAMs to the cellular uropod (del Pozo et al., 1995). Since ERMs have previously been shown to be involved in protrusive membrane phenomena (Tsukita et al., 1997), we decided to explore the possible role of this and related proteins in the redistribution of ICAMs during uropod formation. Flow cytometry analysis of T lymphoblasts stimulated with RANTES and labeled with antibodies to adhesion receptors and ezrin/radixin/moesin showed that these cells expressed high levels of ICAM-3 and CD44 and lower amounts of ICAM-1 (Fig. 1). The expression of ezrin/moesin/radixin ERM proteins was found to be significant, but it was only detected after permeabilization (Fig. 1) since in T lymphocytes these proteins are located intracellularly.

Since time-lapse phase contrast video microscopy revealed that T lymphoblasts stimulated with RANTES are capable of migrating on fibronectin (Fig. 2 *a*), we decided

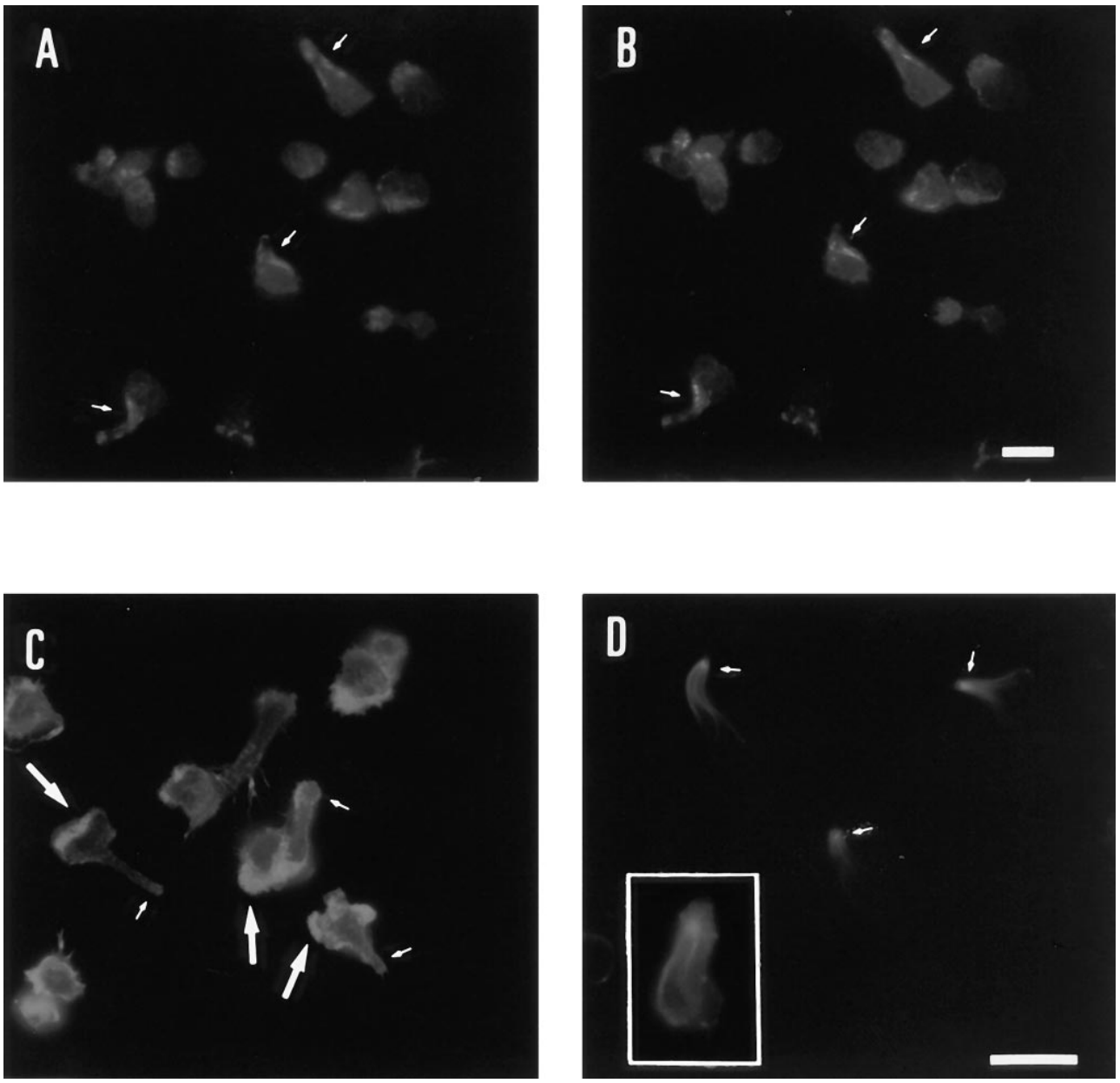

Figure 3. Redistribution of cytoskeletal components to cellular uropods. T lymphoblasts adhered to FN80 were stimulated with RANTES as described in Material and Methods. Then, cells were fixed, permeabilized, and double stained for radixin, pAb 457 (*A*) and myosin II (*B*) or single stained for β-actin (*C*) and α-tubulin (*D*). Small arrows point to neck of uropods in *A* and *B*, whereas in *C* and *D* they point to uropod tips. Large arrows indicate cellular leading edge. Note the close colocalization of radixin and moesin (*A* and *B*) at the uropod neck, the slight stain of β-actin in uropods in contrast to strong stain at the leading edges (*C*), and the presence of nodes of microtubules at the uropod tips (*D*). Inset in *D* shows a magnification of a typical polarized cell stained for α-tubulin. Bar, 10 μm.

to determine whether chemokines can promote redistribution of ERM proteins to the uropod. Immunofluorescence microscopy of T lymphoblasts adhered to the 80-kD fragment of fibronectin in the presence of RANTES showed the formation of the uropod and redistribution of ICAM-3 and -1 to this structure (Fig. 2 *b*, *A* and *B*, respectively). The 13/H9 mAb, which recognizes all three members of the ERM family, showed staining both at leading edges (*large arrow*) and uropod (*small arrows*) (Fig. 2 *c*, *A*). To identify which of the three ERM proteins were localized in uropods, immunofluorescence analysis was performed using antibodies specific for each protein. Ezrin, as previously reported (Egerton et al., 1992; Thuillier et al., 1994), was homogeneously distributed in the cytosol of T cells (Fig. 2 *c*, *B*), whereas moesin was preferentially located at the tip of cellular uropods by staining with the specific mAb 38/87 (Fig. 2 *c*, *C*), which in lymphoblastoid cells only reacts with moesin (Schwartz-Albiez et al., 1995). Double immunofluorescence analysis revealed that radixin showed a pattern of staining identical to that observed for myosin II, colocalizing with linear arrays of myosin II in the neck of uropod (Fig. 3, *A* and *B*).

The localization of other cytoskeletal components such as β-actin and tubulin was also examined in polarized lymphocytes. β-actin was weakly expressed in uropods (Fig. 3 *C*, *small arrows*), but concentrated at leading edges (Fig. 3 *C*, *large arrows*). Interestingly, the staining with an anti–α-tubulin mAb showed the presence of nodes of microtubules in the distal part of the uropod (Fig. 3 *D*, *inset*), which is in accordance with previous reports describing connections between ERM proteins and microtubules (Goslin et al., 1989; Birgbauer et al., 1991).

Chemokines Induce Clustering of Moesin in the Uropod of Polarized Lymphocytes

Since the above results suggested that moesin could be linked to some adhesion receptors that colocalized with it, we decided to study the possible association of these molecules in T lymphoblasts adhered to FN80, in the presence of either polarization-inducing anti–ICAM-3 mAb or chemokines. By double immunofluorescence, we found that moesin and ICAM-3 were evenly distributed on the membrane of unstimulated T lymphoblasts (Fig. 4 *a*, *A* and *B*). Interestingly, cells treated with either anti–ICAM-3 HP2/19 mAb (Fig. 4 *a*, *C* and *D*), RANTES (*E* and *F*), or MCP-1 (*G* and *H*) showed a coincident redistribution of moesin and ICAM-3 to the tips of uropods. To further assess the spatial codistribution of ICAM-3 and moesin, polarized T lymphoblasts adhered to FN80 were double stained with antibodies specific for both molecules, and confocal microscopy was carried out. No ICAM-3 fluorescence and only a weak signal of moesin were found at the substratum level (Fig. 4 *b*, *A* and *D*, respectively). However, upper optical sections showed that the fluorescence of ICAM-3 (Fig. 4 *b*, *B* and *C*) and moesin (Fig. 4 *b*, *E* and *F*) gradually increased, colocalizing in the uropod of the cell. Quantitation of the number of cells with uropods and redistributed ICAM-3 and moesin molecules showed a correlation between presence of uropods and the redistribution of these molecules for both nonstimulated and stimulated T cells (Fig. 4 *c*).

To further analyze the phenomenon of ICAM-3–moesin codistribution, we performed immunofluorescence studies in the T lymphoblast–like cell line HSB-2 (Dougherty et al., 1988), which displays a constitutively polarized morphology. As expected, the molecules ICAM-1 (data not shown), ICAM-3, CD44, and moesin were localized in prominent uropods of these cells without requiring any stimulation (Fig. 5). In contrast, VLA-4 was randomly distributed over the cell surface membrane. In these cells, ICAM-3 was the adhesion molecule most frequently detected in uropods since it was found in 80% of uropod-bearing cells, whereas CD44 and ICAM-1 were detected in only 40% of uropod-bearing cells.

Interaction of Moesin with ICAM-3 in T Lymphocytes

To determine whether moesin directly interacts with ICAM-3, cell lysates from T lymphoblasts, either nonstimulated or stimulated (anti-ICAM-3 HP2/19 mAb, RANTES), were immunoprecipitated with mAb against several adhesion molecules concentrated (CD44, ICAM-1, and ICAM-3) or not (VLA-4) in uropods, transferred to nitrocellulose membranes, and blotted with an antimoesin pAb (Fig. 6, *A* and *B*). Coprecipitation of moesin was observed with mAb against ICAM-3 (Fig. 6 *A*, lanes *1–3*) and CD44 (Fig. 6 *B*, lanes *1–3*). In contrast, no significant amounts of moesin were found in the anti–VLA-α4 (Fig. 6 *A*, lanes *5–7*) and the anti–ICAM-1 (Fig. 6 *B*, lanes *5–7*) precipitates.

The association of moesin with adhesion molecules was also studied in HSB-2 cells by immunoprecipitation and Western blot analysis (Fig. 7 *A*). As observed in T lymphoblasts, moesin was clearly appreciated in the anti–ICAM-3 precipitate (Fig. 7 *A*, lane *3*). Small amounts of moesin were also detected in precipitates with anti-CD44 (Fig. 7 *A*, lane *4*), whereas no moesin signal was observed in precipitates corresponding to VLA-4 and ICAM-1 (lanes *1* and *2*, respectively). These data indicate that moesin is associated to ICAM-3 in these constitutively polarized T cells.

Studies on the association between ICAM-3 and moesin in different T cell preparations indicated that moesin also associated with ICAM-3 in peripheral blood T lymphocytes, but to a lower extent than in T lymphoblasts and the HSB-2 T cell line (Fig. 7 *B*, lanes *5–7*, respectively). No significant amounts of moesin were found in the anti–VLA-4 precipitates (Fig. 7 *B*, lanes *1–3*).

Interaction of the Cytoplasmic Tail of ICAM-3 with Moesin

To further investigate the ICAM-3–moesin interaction, we performed precipitation studies with a GST fusion protein containing the ICAM-3 cytoplasmic region (Fig. 8 *A*). We found that the GST–CyICAM-3 fusion protein specifically precipitated, from metabolically labeled Jurkat T cell lysates, a prominent single band of 78 kD, whereas no protein bands were observed in precipitates from GST-CyCD148 or control GST (Fig. 8 *B*). Western blot analysis carried out in parallel demonstrated that the 78-kD protein bound to GST–CyICAM-3 corresponded to moesin (Fig. 8 *C*). These results indicate that the cytoplasmic tail of ICAM-3 directly interacts with moesin.

Polarization of T Cells and Moesin–ICAM-3 Association Are Interrelated Events

The results shown above (Figs. 4–7) strongly suggested that there is a close correlation between the clustering of adhesion receptors, the localization and concentration of moesin in the uropod, and the amount of moesin that was found to be complexed with ICAM-3. Densitometric analysis showed that significantly higher amounts of moesin coprecipitated with ICAM-3 and CD44 when the cells were treated with agents that induce cell polarization, such as the anti–ICAM-3 mAb or the chemokine RANTES, compared to untreated lymphoblasts (Fig. 6, *C* and *D*). To further investigate this issue, we used the myosin-disrupting drug butanedione monoxime, which prevents lymphocyte polarization and uropod formation. Pretreatment of RANTES-stimulated T lymphoblasts with this drug abolished cell polarization and prevented uropod formation and redistribution of ICAM-3 and moesin (Fig. 9 *a*). Interestingly, butanedione monoxime also diminished the association of moesin with ICAM-3 as determined by Western blot analysis (Fig. 9, *b* and *c*). These results strongly suggest that the association of ICAM-3 with moesin increases

a

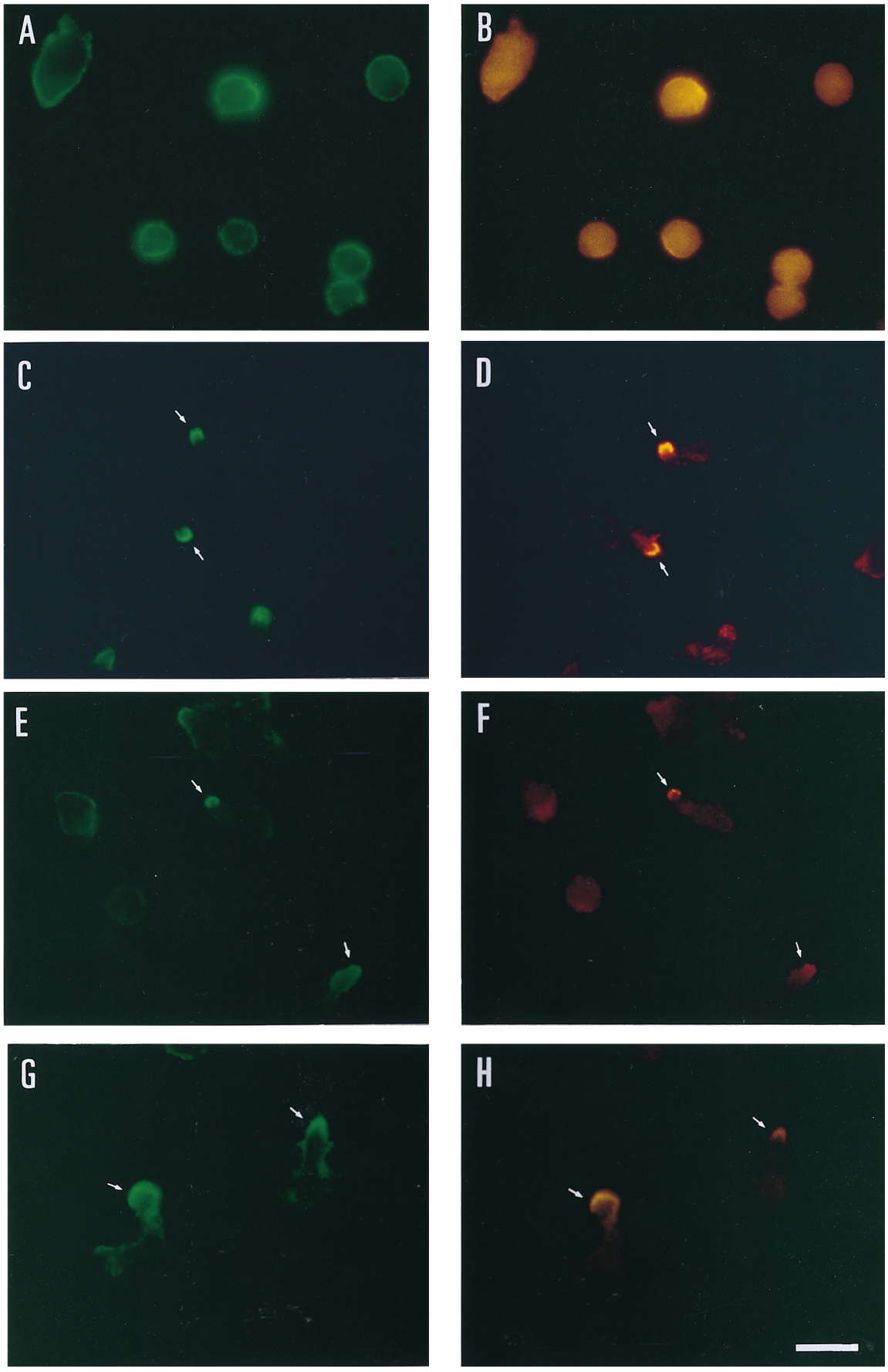

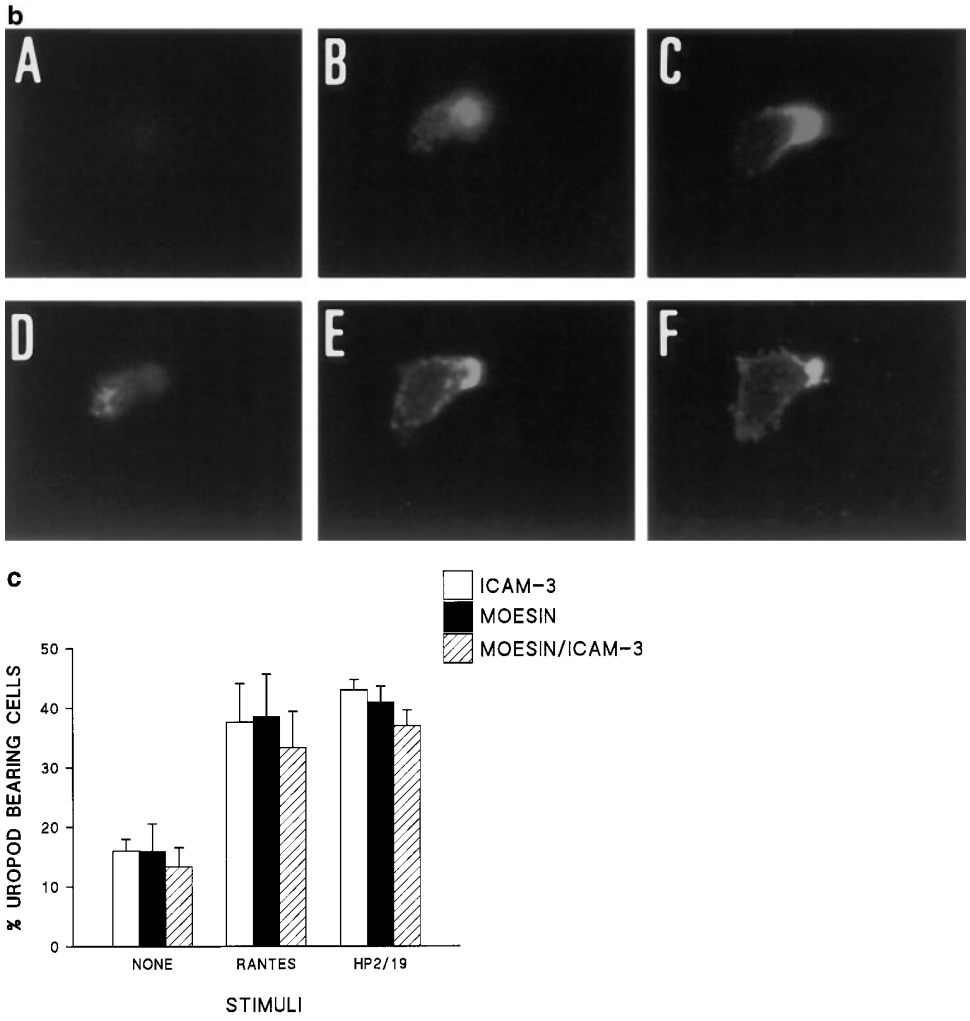

Figure 4. Moesin colocalized with ICAM-3 at the uropods of T lymphoblasts. (*a*) T lymphoblasts adhered to FN80 either nonstimulated (*A* and *B*) or stimulated with the anti–ICAM-3 mAb HP2/19 (*C* and *D*), RANTES (*E* and *F*), or MCP-1 (*G* and *H*) were double stained for moesin, mAb 38/37 (*A*, *C*, *E*, and *G*, *green fluorescence*), and for ICAM-3, mAb TP1/25 (*B*, *D*, *F*, and *H*, *red fluorescence*). Small arrows point to the tip of the cellular uropods. (*b*) Confocal microscopy analysis of cell distribution of ICAM-3 and moesin. T lymphoblasts adhered to FN80 in the presence of the uropod-inducing HP2/19 mAb were double stained for ICAM-3 (*A*, *B*, and *C*) and moesin (*D*, *E*, and *F*) as described under Materials and Methods. Optical sections were adjusted at substratum level (*A* and *D*), 1.8 μm (*B* and *E*), and 3.6 μm upper (*C* and *F*). Colocalization in the cellular uropod of ICAM-3 (intense green fluorescence in *B* and *C*) and moesin (intense red fluorescence in *E* and *F*) is observed at upper levels. (*c*) T lymphoblasts, unstimulated and stimulated with RANTES (or the mAb HP2/19) were double stained for moesin and ICAM-3, and the percent of cells in which these molecules were concentrated in uropods was quantified as described in Materials and Methods. The arithmetic mean ± SD of four independent experiments with T lymphoblasts from four different donors is shown. Bar, 10 μm.

during the clustering of these molecules to the uropod in the process of cell polarization.

Discussion

Lymphocyte activation induces rapid modifications of cell membrane that result in redistribution of several surface molecules and formation of new structures that change cell morphology to a polarized shape. These changes play an important role in cell–cell interactions and migration of immune cells towards inflammatory sites. We have previously reported that chemotactic cytokines induce lymphocyte polarization with redistribution of adhesion molecules (ICAM-1, ICAM-3, and CD44) to a cell uropod of the migrating lymphocyte (del Pozo et al., 1995). The cytoskeletal-binding proteins ezrin, radixin, and moesin seem to be involved in formation of dynamic cell membrane structures by linking cytoskeletal components with membrane integral proteins (Sato et al., 1992). In this study, we searched for ERM proteins that could associate with ICAM-3 and other adhesion molecules in uropods of polarized T lymphocytes induced with chemokines.

Our results indicate that T lymphocyte uropods are specialized cell structures in which CD44, ICAM-1, and ICAM-3 adhesion molecules are redistributed preferentially and in which the cytoskeletal elements myosin II and microtubules are packed. Interestingly, we have found that whereas β-actin–containing microfilaments are the main cytoskeletal elements in the cell leading edge, in the uropod these filaments are almost excluded. It is well established that filaments of actin and tubulin are required for intracellular traffic through interaction with motor proteins (Skoufias and Scholey, 1993), while actin plays a central role in cell motility (Cramer et al., 1994). The enhanced localization of microtubules compared to microfilaments in uropods are in agreement with functional studies that indicate that these cellular protrusions are involved in cell–cell interactions and leukocyte recruitment rather than in cellular locomotion (del Pozo et al., 1997).

Our results using the mAb 13/H9, which recognizes each of the ERM proteins as well as the protein associated with neurofibromatosis 2, merlin (Winckler et al., 1994), show staining at both the leading edge and the uropod, with moesin and radixin detected in the uropod of these cells.

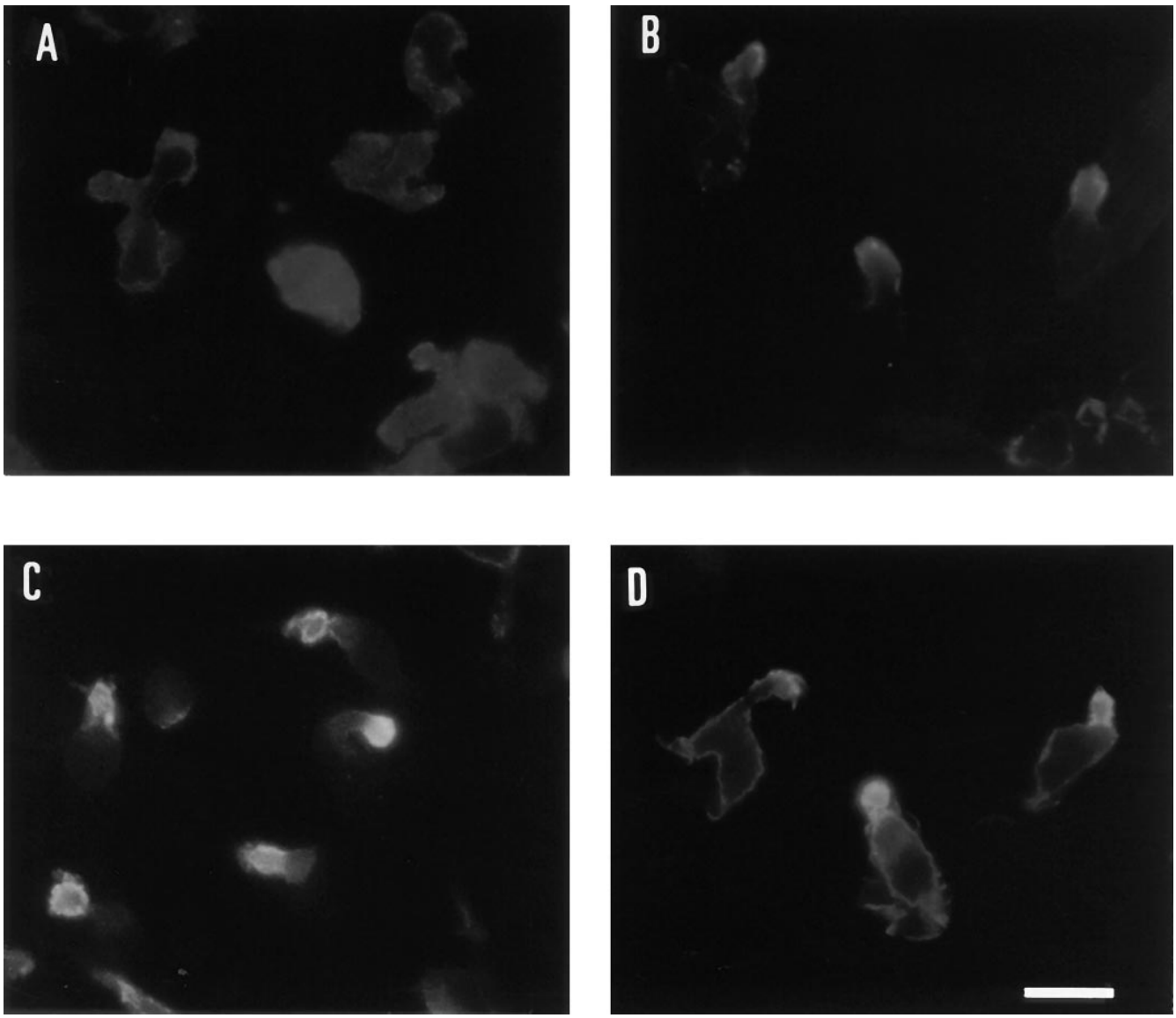

Figure 5. Localization of moesin and ICAM-3 in uropods of HSB-2 cells. HSB-2 cells were adhered to coverslips coated with FN80 at 20 μg/ml for 30 min, fixed with 4% paraformaldehyde, and stained for VLA-4, mAb HP2/1 (*A*), CD44, mAb HP2/9 (*B*), ICAM-3 mAb TP1/25, and moesin mAb 38/37 (*D*). Moesin staining was performed after cell permeabilization with 0.1% Triton X-100 for 15 min. Bar, 10 μm.

Moesin decorated the tip of cellular uropodia and colocalized with adhesion molecules ICAM-1, ICAM-3, and CD44, whereas radixin colocalized with arrays of myosin II at the uropod neck. Contradictory data have been reported about the localization of moesin in plasma membrane; whereas some studies described that this protein is an externally exposed membrane receptor for measles virus in human peripheral blood mononuclear cells and other blood cell lines (Dunster et al., 1994), other works carried out with different cell models of virus infection have documented that ERM proteins are located intracellularly and associated with cytoplasmic tails of integral proteins (Sagara et al., 1995). Our data indicate that moesin is indeed localized at the inner side of the plasma membrane of T lymphoblasts, as demonstrated by both immunofluorescence microscopy and flow cytometry using specific polyclonal and monoclonal antibodies. Taking into account the proximity of moesin and microtubules in the uropods, it is tempting to speculate that moesin could be interacting with microtubules in this cellular domain. In this regard, it has been proposed that an ERM protein recognized by 13/H9 mAb interacts with actin in growth cones and microtubules of axons in neuronal cells (Goslin et al., 1989; Birgbauer et al., 1991).

Our data demonstrate a physical association between the intracellular protein moesin and the transmembrane adhesion molecules ICAM-3 and CD44. Moreover, the coprecipitation studies with the GST–CyICAM-3 fusion protein demonstrate a direct interaction between moesin and the cytoplasmic region of ICAM-3. In this regard, a larger amount of moesin was associated in T lymphoblasts or HSB-2 T cells as compared to nonstimulated peripheral

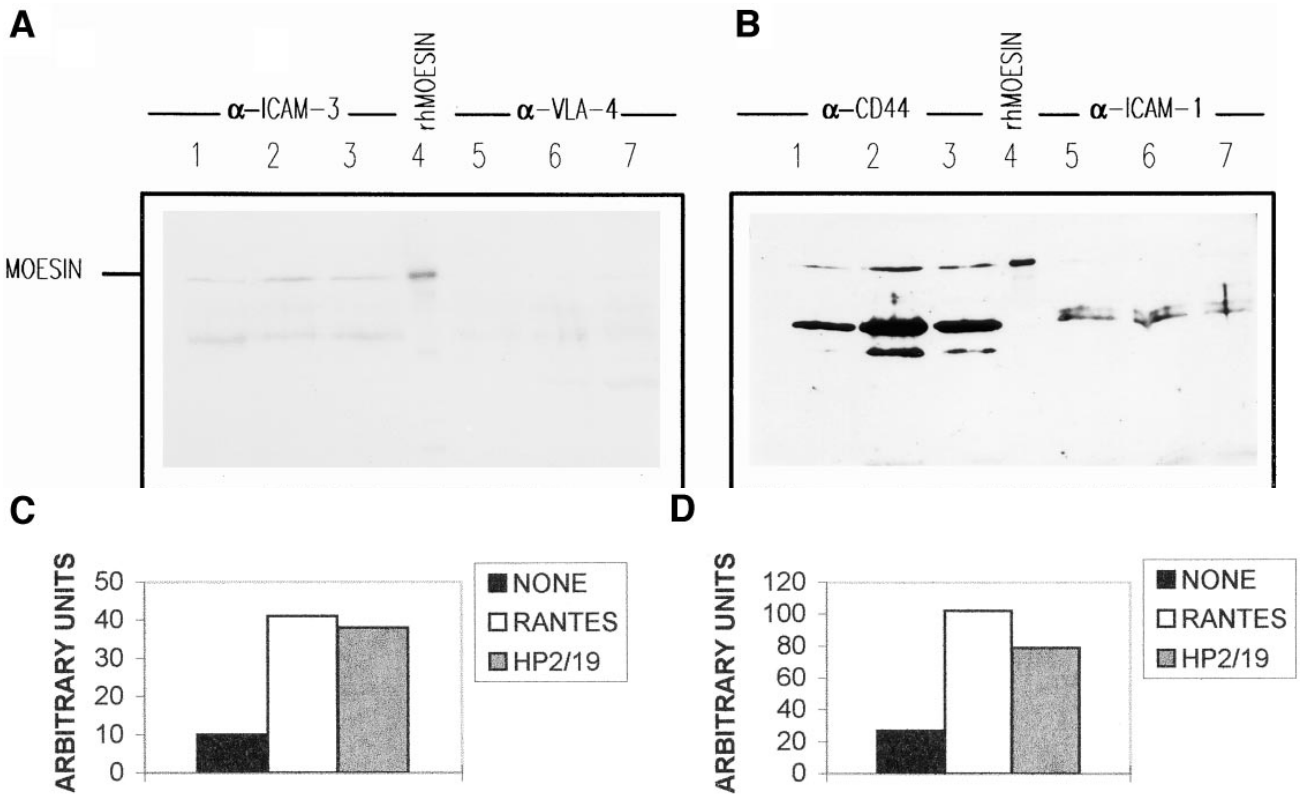

Figure 6. Association of moesin with ICAM-3 and CD44 in polarized T lymphoblasts. T cells adhered to FN80 (lanes *1* and *5*) were stimulated with RANTES (lanes *2* and *6*) or anti–ICAM-3 mAb HP2/19 (lanes *3* and *7*) for 30 min. Cells were then lysed and solubilized with RIPA buffer. Soluble fractions were immunoprecipitated with anti–ICAM-3 mAb TP1/25 (*A*, lanes *1–3*), anti–VLA-4 mAb HP2/1 (*A*, lanes *5–7*), anti-CD44 mAb HP2/9 (*B*, lanes *1–3*), and anti–ICAM-1 mAb Hu5/3 (*B*, lanes *5–7*). Human recombinant moesin standard was added to lanes *4.* Each immunoprecipitate as well as standard were immunoblotted with antimoesin pAb 95/2 after 7.5% SDS-PAGE. The lower bands correspond to mouse Igs from different mAbs used. (*C* and *D*) Densitometric analysis of moesin bands coprecipitated with ICAM-3 (*A*, lanes *1–3*, and *C*) and with CD44 (*B*, lanes *1–3*, and *D*). In *C*, the values in arbitrary units of moesin bands corresponding to immunoprecipitates from cells nonstimulated or stimulated with RANTES or anti–ICAM-3 HP2/19 were 10.12, 41.33, and 38.22, respectively. In *D* the values were 27.33, 102.19, and 79.80, respectively.

blood lymphocytes. In addition, agents that induce cell polarization, such as the chemokines RANTES and MCP-1, as well as the anti–ICAM-3 mAb HP2/19, increase the degree of association between moesin and ICAM-3 in uropods of T lymphocytes. We have also found that the adhesion molecule CD44 is associated with moesin in T lymphocytes. In this regard, the 140-kD isoform of CD44 has been reported previously to be complexed with ezrin, radixin, and moesin in BHK and L cells (Tsukita et al., 1994). Although no evidence of association of ICAM-1 and VLA-4 with moesin was found in either T lymphoblasts or HSB-2 cells, previous studies have shown that both molecules are associated with α-actinin; ICAM-1 interacts with this protein through its cytoplasmic domain in uropods of lymphoblastoid B cell lines (Carpén et al., 1992), whereas VLA-4 interacts through the β1 chain (Otey et al., 1990). Since expression of ICAM-1 is about 10-fold lower than ICAM-3 and CD44 in T lymphoblasts and HSB-2 cells, the inability to detect such low levels of ICAM-1–moesin association does not rule out the possibility that these interactions still exist.

It is well known that chemokines are able to induce chemotaxis, adhesion to extracellular matrix, and costimulation of T lymphocytes among other biologic activities (Lloyd et al., 1996; Taub et al., 1996). Our findings indicate that they also regulate the association of moesin with ICAM-3 and CD44 in uropods, a phenomenon that appears to be related to the induction of lymphocyte polarization by these cytokines. This is supported by results with the constitutively polarized HSB-2 T cells, in which moesin was found to be associated with ICAM-3, and to a lower extent with CD44. This molecular interaction thus appears to be related to the degree of cell polarity, which is high in HSB-2 cells and in lymphoblasts and low in peripheral blood lymphocytes. Furthermore, the inhibitory effect of the myosin-disrupting drug on moesin redistribution and moesin–ICAM-3 association further suggests the relationship between these phenomena and cell polarization. Together with the localization of myosin II in the neck of the uropod, where it colocalizes with radixin, these results suggest that myosin could be important in uropod formation and for development of cell polarity in T lymphocytes. This is in agreement with previous suggestions that conventional myosins generate force for membrane

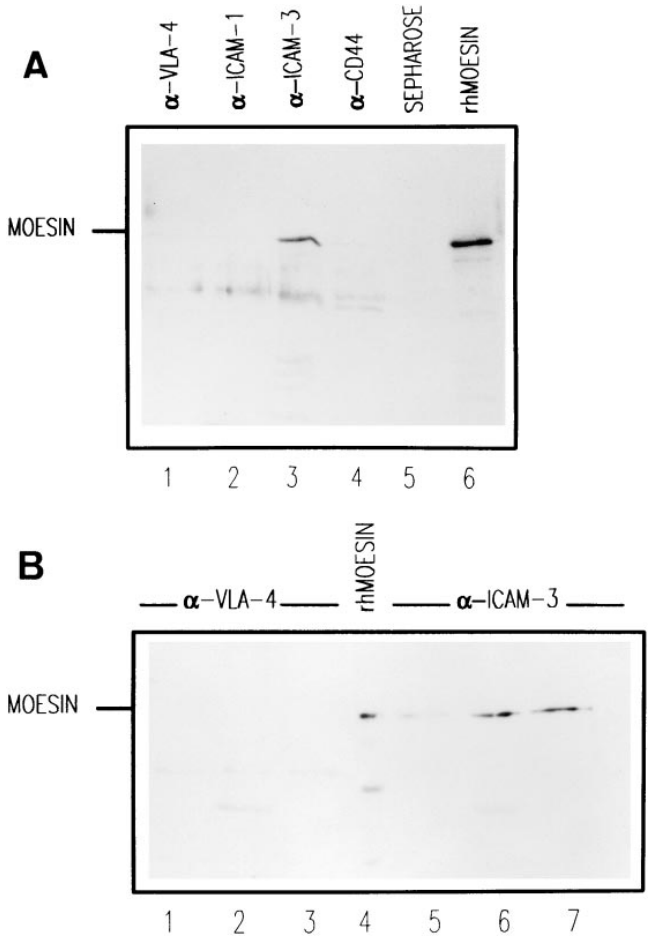

Figure 7. Coimmunoprecipitation of moesin with ICAM-3 in HSB-2 cells and peripheral blood lymphocytes. (*A*) HSB-2 cell lysates were immunoprecipitated with the anti–VLA-4, HP2/1 (lane *1*), anti–ICAM-1, Hu5/3 (lane *2*), anti–ICAM-3, TP1/25 (lane *3*), and anti-CD44, HP2/9 mAbs (lane *4*) as well as Sepharose beads (lane *5*). Each immunoprecipitate as well as a standard of human recombinant moesin (lane *6*) were immunoblotted with antimoesin pAb 95/2 after 7.5% SDS-PAGE. (*B*) Coimmunoprecipitation of moesin with ICAM-3 in T cells with different polarity. Peripheral blood lymphocytes (lanes *1* and *5*), T lymphoblasts (lanes *2* and *6*), or HSB-2 cells (lanes *3* and *7*) were lysed and solubilized with RIPA buffer, and the soluble fraction was immunoprecipitated for VLA-4, mAb HP2/1 (lanes *1–3*) and for ICAM-3, mAb TP1/25 (lanes *5–7*). Human recombinant moesin was loaded in lane *4.* Each immunoprecipitate as well as standard were immunoblotted with antimoesin pAb 95/2 after 7.5% SDS-PAGE.

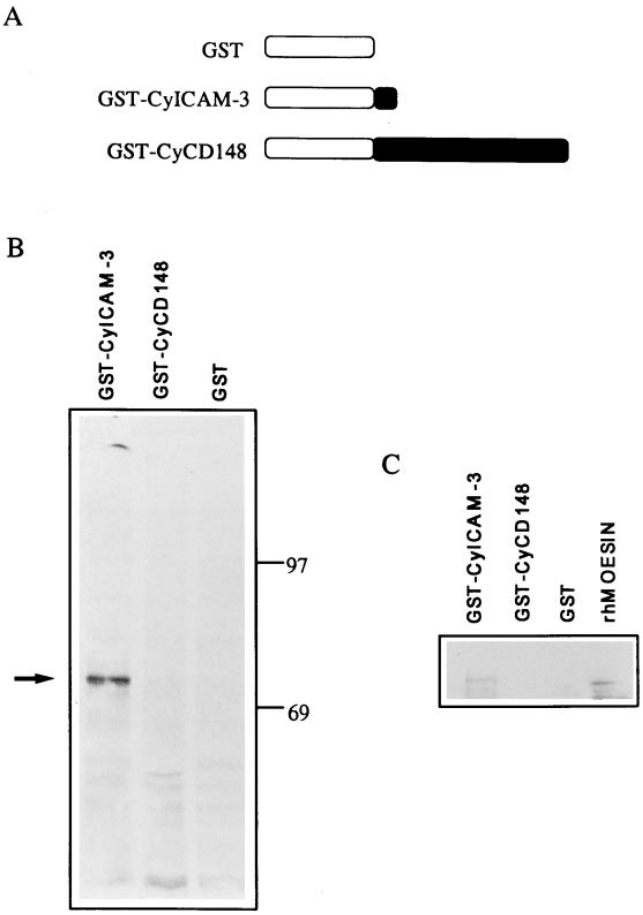

Figure 8. Interaction of the cytoplasmic region of ICAM-3 with moesin from Jurkat cell lysates. (*A*) Schematic representation of the GST, GST–CyICAM-3, and GST–CyCD148 fusion proteins used in this analysis. (*B*) Specific association of a 78-kD protein with GST–CyICAM-3 from metabolically labeled cells. Jurkat cells were metabolically labeled and lysed. After discarding cell debris and nuclei, supernatants were collected and allowed to bind to equivalent amounts of GST, GST–CyICAM-3, and GST–CyCD148 proteins bound to glutathione Sepharose 4B beads by overnight incubation at 4°C. Bound proteins were sequentially washed with lysis buffer containing 0.1% SDS and 0.65 M NaCl and then subjected to 8% SDS-PAGE. Before drying, the gel was incubated for 30 min in Amplify solution (Amersham Corp.). Molecular masses in kilodaltons are indicated at the right; the arrow indicates the position of the 78-kD protein bound to the GST–CyICAM-3 fusion protein. (*C*) Precipitates from unlabeled Jurkat cells were carried out as in *B*, SDS-PAGE separated, and immunoblotted with the antimoesin pAb 95/2. Recombinant human moesin was also included as control.

Figure 9. Effect of butanedione monoxime on both moesin redistribution to the uropod and its association with ICAM-3. T lymphoblasts preincubated with 10 mM butanedione monoxime were allowed to adhere to coverslips coated with FN80 and then stimulated with 10 ng/ml RANTES. (*a*) Cells were stained for ICAM-3 (*A* and *B*) and moesin (*C* and *D*) in the presence (*B* and *D*) or not (*A* and *C*) of butanedione monoxime. (*b*) In experiments run in parallel, cell lysates from butanedione monoxime–treated (lane *4*) or untreated cells (lanes *2* and *3*) were immunoprecipitated for ICAM-3 (mAb TP1/25), and moesin was detected by using the pAb 95/2 after 7.5% SDS-PAGE. Purified recombinant moesin was added in lane *1.* The lower bands correspond to mouse Igs from the mAb used in the immunoprecipitation. *R*, RANTES; *BM*, butanedione monoxime. (*c*) Densitometric analysis of bands corresponding to moesin in *b.* The values in arbitrary units corresponding to bands of moesin coprecipitated with anti–ICAM-3 from cells treated with either RANTES at 10 ng/ml, at 5 ng/ml, or at 10 ng/ml plus 10 mM butanedione monoxime were 108.11, 65.32 and 25.00, respectively. Bar, 10 μm.

a

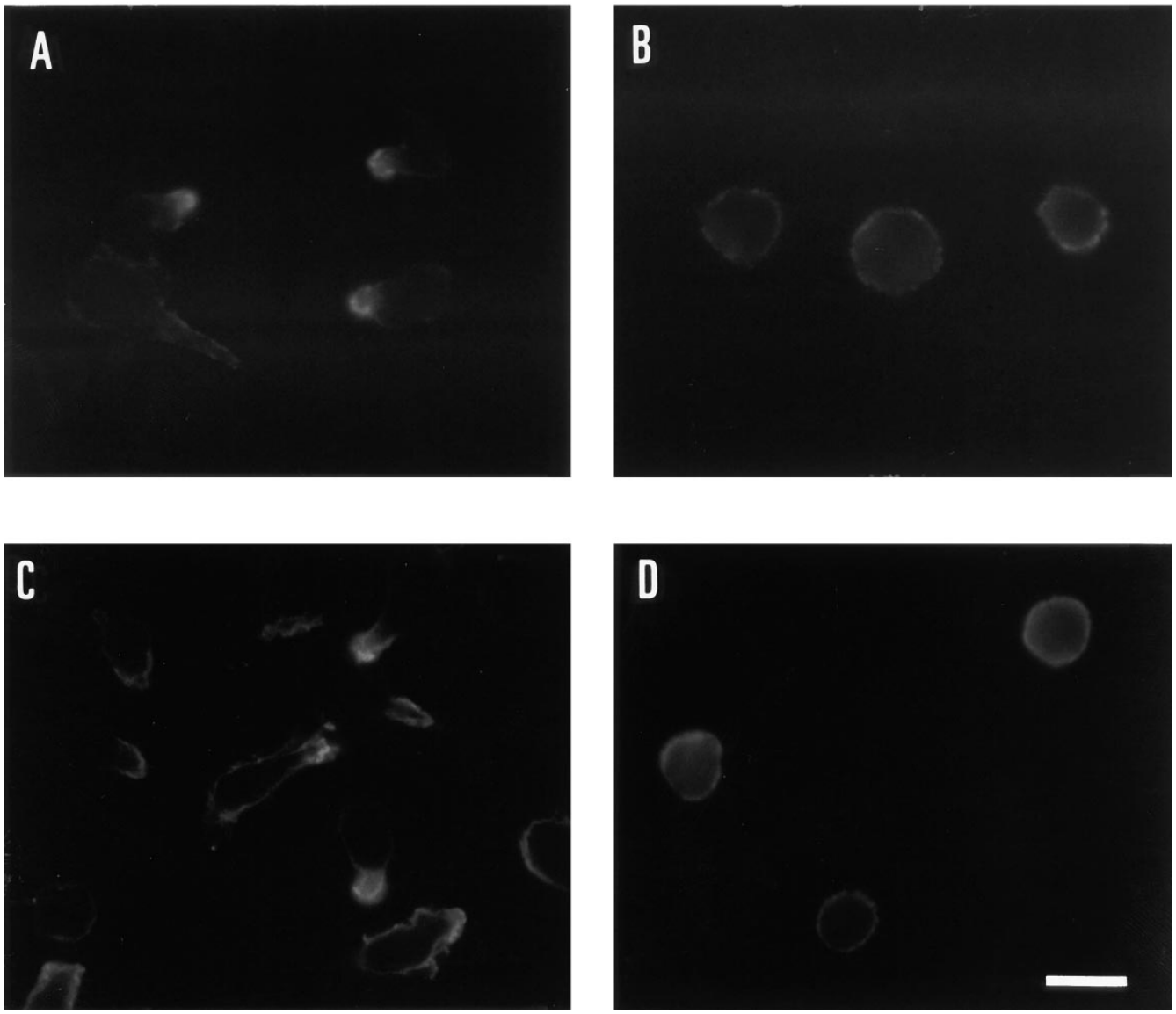
A
B
C
D

b

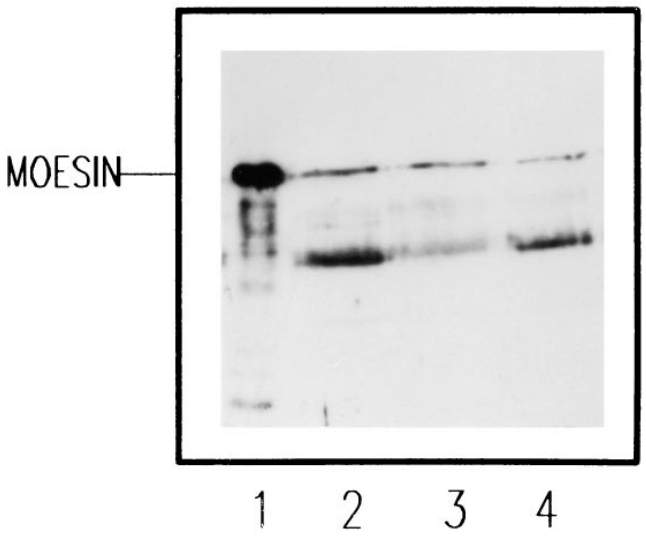
MOESIN
1
2
3
4

c

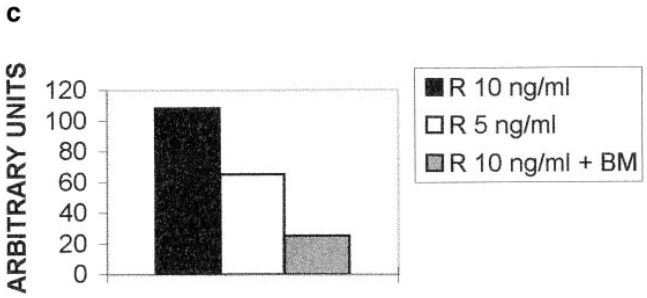
ARBITRARY UNITS
120
100
80
60
40
20
0
R 10 ng/ml
R 5 ng/ml
R 10 ng/ml + BM

protrusion (Condeelis, 1993) and for driving contractile processes that move surface receptors into a cap (Pasternak et al., 1989).

There is additional evidence suggesting that members of the ERM family drive the redistribution of membrane receptors. Mouse thymoma cells transfected with ezrin cDNA display a uropod where ICAM-2 is concentrated, and this ezrin-driven cellular localization of ICAM-2 seems to play a role in the NK-mediated cell lysis of these target cells (Helander et al., 1996). A possible mechanism is suggested by experiments with human platelets. Upon activation with thrombin, platelets spread and change their shape by forming long moesin-containing filopodia. During this process, moesin is phosphorylated at residue Thr 558, which is located close to a binding site for F-actin (Nakamura et al., 1995). It is possible that a similar regulatory process operates during activation of lymphoid cells, where moesin association with ICAM-3 is induced.

Based on our observations, we postulate that the binding of chemokines to their receptors triggers both contraction of myosin and association of moesin with ICAM-3. This association could be mediated by Rho, as it has recently been proposed for CD44–moesin interaction in other cells (Hirao et al., 1996). Since moesin is evenly distributed at the inner side of plasma membrane in unstimulated lymphocytes, it is feasible that after chemokine stimulation, moesin dissociates from unknown proteins, interacting then with both ICAM-3 and cytoskeletal elements. In this regard, a similar mechanism of reversible association has recently been described for uPAR and Mac-1/p150, 95 integrins in uropods of neutrophils (Petty and Todd, 1996). On the other hand, it is also feasible that myosin contraction promotes clustering and redistribution of moesin–ICAM-3 complexes together with the narrowing of the cell at the level of uropod neck. The inherent polarity of MTOC in the vicinity of the membrane nucleus in resting T cells would determinate the site of uropod formation and final localization of moesin–ICAM-3 complexes by direct or indirect interaction with microtubules. A similar model might apply to CD44. This hypothetical model raises interesting questions concerning the signaling pathways that connect chemokine receptor with moesin.

We thank Drs. R. González-Amaro, P. Lauzurica (Hospital de la Princesa, Madrich), and F.W. Luscinskas, (Harvard Medical School, Boston MA) for critical readings of the manuscript. We are gratefully indebted to P. Sánchez-Mateos, M. Nieto, M. Yáñez, and A. Roca for their help and advice with different techniques.

This work was supported by grants SAF96/0039 from Plan Nacional de Investigación y Desarrollo, 07/44/96 from Comunidad Autónoma de Madrid, and from Fundación Científica de la Asociación Española contra el Cancer (to F. Sánchez-Madrid), and grants from the National Institute of Health (AR 41045) and the Tobacco Related Disease Research Program (TRDRP 4RT-0316) to H. Furthmayr, and by fellowship BAE FIS 96/5357 to M.A. del Pozo.

Received for publication 21 February 1997 and in revised form 29 May 1997.

References

Amieva, M.R., and H. Furthmayr. 1995. Subcellular localization of moesin in dynamic filopodia, retraction fibers, and other structures involved in substrate exploration, attachment, and cell-cell contacts. *Exp. Cell Res.* 219:180–196.

Arpin, M., M. Algrain, and D. Louvard. 1994. Membrane-actin microfilament connections: an increasing diversity of players related to band 4.1. *Curr. Opin. Cell Biol.* 6:136–141.

Berryman, M., R. Gary, and A. Bretscher. 1995. Ezrin oligomers are major cytoskeletal components of placental microvilli: a proposal for their involvement in cortical morphogenesis. *J. Cell Biol.* 131:1231–1242.

Birgbauer, E., and F. Solomon. 1989. A marginal band-associated protein has properties of both microtubule- and microfilament-associated proteins. *J. Cell Biol.* 109:1609–1620.

Birgbauer, E., J.H. Dinsmore, B. Winkler, A.D. Lander, and F. Solomon. 1991. Association of ezrin isoforms with the neuronal cytoskeleton. *J. Neurosci. Res.* 30:232–241.

Bretscher, A. 1993. Microfilaments and membranes. *Curr. Opin. Cell Biol.* 5: 653–660.

Campanero, M.R., R. Pulido, J.L. Alonso, J.P. Pivel, F.X. Pimentel-Muiños, M. Fresno, and F. Sánchez-Madrid. 1991. Down-regulation by tumor necrosis factor alpha of neutrophil cell surface expression of the sialophorin CD43 and the hyaluronate receptor CD44 through a proteolytic mechanism. *Eur. J. Immunol.* 21:3045–3048.

Campanero, M.R., M.A. del Pozo, A.G. Arroyo, P. Sanchez-Mateos, T. Hernandez, A. Craig, R. Pulido, and F. Sánchez-Madrid. 1993. ICAM-3 interacts with LFA-1 and regulates the LFA-1/ICAM-1 cell adhesion pathway. *J. Cell Biol.* 123:1007–1016.

Campanero, M.R., P. Sánchez-Mateos, M.A. del Pozo, and F. Sánchez-Madrid. 1994. ICAM-3 regulates lymphocyte morphology and integrin-mediated T cell interaction with endothelial cell and extracellular matrix ligands. *J. Cell Biol.* 127:867–878.

Carpén, O., P. Pallai, D.E. Staunton, and T.A. Springer. 1992. Association of Intercellular adhesion molecule-1 (ICAM-1) with actin-containing cytoskeleton and α-actinin. *J. Cell Biol.* 118:1223–1234.

Condeelis, J. 1993. Life at the leading edge: the formation of cell protrusions. *Annu. Rev. Cell Biol.* 9:411–444.

Crabtree, G.R., and N.A. Clipstone. 1994. Signal transmission between the plasma membrane and nucleus of T lymphocytes. *Annu. Rev. Biochem.* 63: 1045–1083.

Cramer, L.P., T.J. Mitchinson, and J.A. Theriot. 1994. Actin-dependent motile forces and cell motility. *Curr. Opin. Cell Biol.* 6:82–86.

del Pozo, M.A., P. Sánchez-Mateos, M. Nieto, and F. Sánchez-Madrid. 1995. Chemokines regulate cellular polarization and adhesion receptor redistribution during lymphocyte interaction with endothelium and extracellular matrix. Involvement of cAMP signaling pathway. *J. Cell Biol.* 131:495–508.

del Pozo, M.A., C. Cabañas, M.C. Montoya, A. Ager, P. Sánchez-Mateos, and F. Sánchez-Madrid. 1997. ICAMs redistributed by chemokines to cellular uropods as a mechanism for recruitment of T lymphocytes. *J. Cell Biol.* 137: 493–508.

Dougherty, G.J., S. Murdoch, and N. Hogg. 1988. The function of human intercellular adhesion molecule-1 (ICAM-1) in the generation of an immune response. *Eur. J. Immunol.* 18:35–39.

Dunster, L.M., J. Schneider-Schaulies, S. Löffler, W. Lankes, R. Schwartz-Albiez, F. Lottspeich, and V.T. Meulen. 1994. Moesin: a cell membrane protein linked with susceptibility to measles virus infection. *Virology.* 198:265–274.

Egerton, M., W.H. Burgess, D. Chen, B.J. Druker, A. Bretscher, and L.E. Samelson. 1992. Identification of ezrin as an 81-KD tyrosine-phosphorylated protein in T cells. *J. Immunol.* 149:1847–1852.

Fath, K.R., and D.R. Burgess. 1995. Not actin alone. *Curr. Biol.* 5:591–593.

Goslin, K., E. Birgbauer, G. Banker, and F. Solomon. 1989. The role of cytoskeleton in organizing growth cones: a microfilament-associated growth cone component depends upon microtubules for its localization. *J. Cell Biol.* 109:1621–1631.

Helander, T.S., O. Carpén, O. Turunen, P.E. Kovanen, A. Vaheri, and T. Timonen. 1996. ICAM-2 redistributed by ezrin as a target for killer cells. *Nature (Lond.).* 382:265–268.

Hirao, M., N. Sato, T. Kondo, S. Yonemura, M. Monden, T. Sasaki, Y. Takai, S. Tsukita, and S. Tsukita. 1996. Regulation mechanism of ERM (ezrin/radixin/moesin) protein/plasma membrane association: possible involvement of phosphatidylinositol turnover and Rho-dependent signaling pathway. *J. Cell Biol.* 135:37–51.

Hitt, A.L., and E.J. Luna. 1994. Membrane interactions with the actin cytoskeleton. *Curr. Biol.* 6:120–130.

Kupfer, A., S.J. Singer, and G. Dennert. 1986. On the mechanism of unidirectional killing in mixtures of two cytotoxic T lymphocytes. Unidirectional polarization of cytoplasmic organelles and the membrane-associated cytoskeleton in the effector cell. *J. Exp. Med.* 163:489–498.

Kupfer, A., T.R. Mosmann, and H. Kupfer. 1991. Polarized expression of cytokines in cell conjugates of helper T cells and splenic B cells. *Proc. Natl. Acad. Sci. USA.* 88:775–779.

Kupfer, H., C.R.F. Monks, and A. Kupfer. 1994. Small splenic B cells that bind to antigen-specific T helper (Th) cells and face the site of cytokine production in the Th cells selectively proliferate: immunofluorescence microscopy studies of Th-B antigen-presenting cell interactions. *J. Exp. Med.* 179:1507–1515.

Lankes, W., A. Griesmacher, J. Grünwald, R. Schwartz-Albiez, and R. Keller. 1988. A heparin-binding protein involved in inhibition of smooth-muscle cell proliferation. *Biochem. J.* 251:831–842.

Lankes, W.T., and H. Furthmayr. 1991. Moesin: a member of the protein 4.1-talin-ezrin family of proteins. *Proc. Natl. Acad. Sci. USA.* 88:8297–8301.

Lloyd, A.R., J.J. Oppenheim, D.J. Kelvin, and D.D. Taub. 1996. Chemokines regulate T cell adherence to recombinant adhesion molecules and extracellular matrix proteins. *J. Immunol.* 156:932–938.

Nakamura, F., M.R. Amieva, and H. Furthmayr. 1995. Phosphorylation of threonine 558 in the carboxyl-terminal actin-binding domain of moesin by thrombin activation of human platelets. *J. Biol. Chem.* 270:31377–31385.

Negulescu, P.A., T.B. Krasieva, A. Khan, H.H. Kerschbaum, and M.D. Cahalan. 1996. Polarity of T cell shape, motility, and sensitivity to antigen. *Immunity.* 4:421–430.

Nieto, M., M.A. del Pozo, and F. Sánchez-Madrid. 1996. Interleukin-15 induces adhesion receptor redistribution in T lymphocytes. *Eur. J. Immunol.* 26: 1302–1307.

Nieto, M., J.M. Frade, D. Sancho, M. Mellado, C. Martinez-A and F. Sánchez-Madrid. 1997. Polarization of chemokine receptors to the leading edge during lymphocyte chemotaxis. *J. Exp. Med.* 186:153–158.

Otey, C.A., F.M. Pavalko, and K. Burridge. 1990. An interaction between α-actinin and the β1 integrin subunit in vitro. *J. Cell Biol.* 111:721–729.

Pasternak, C., J.A. Spudich, and E.L. Elson. 1989. Capping of surface receptors and concomitant cortical tension are generated by conventional myosin. *Nature (Lond.).* 341:549–551.

Petty, H.R., and R.F. Todd. 1996. Integrins as promiscuous signal transduction devices. *Immunol. Today* 17:209–211.

Pulido, R., M.J. Elices, M.R. Campanero, L. Osborn, S. Schiffer, A. Garcia-Pardo, R. Lobb, M.E. Hemler, and F. Sánchez-Madrid. 1991. Functional evidence for three distinct and independent inhibitable adhesion activities mediated by the human integrin VLA-4. *J. Biol. Chem.* 266:10241–10245.

Sagara, J., S. Tsukita, S. Yonemura, S. Tsukita, and A. Kawai. 1995. Cellular actin-binding ezrin-radixin-moesin (ERM) family proteins are incorporated into the rabies virion and closely associated with viral envelope proteins in the cell. *Virology.* 206:485–494.

Sánchez-Mateos, P., M.R. Campanero, M.A. del Pozo, and F. Sánchez-Madrid. 1995. Regulatory role of CD43 leukosialin on integrin-mediated T-cell adhesion to endothelial and extracellular matrix ligands and its polar redistribution to a cellular uropod. *Blood.* 86:2228–2239.

Sato, N., N. Funayama, A. Nagafuchi, S. Yonemura, S. Tsukita, and S. Tsukita. 1992. A gene family consisting of ezrin, radixin and moesin. Its specific localization at actin filament/plasma membrane association sites. *J. Cell Sci.* 103: 131–143.

Schwartz-Albiez, R., A. Merling, H. Spring, P. Möller, and K. Koretz. 1995. Differential expression of the microspike-associated protein moesin in human tissues. *Eur. J. Cell Biol.* 67:189–198.

Skoufias, D.A., and J.M. Scholey. 1993. Cytoplasmic microtubule-based motor proteins. *Curr. Opin. Cell Biol.* 5:95–104.

Takeuchi, K., N. Sato, H. Kasahara, N. Funayama, A. Nagafuchi, S. Yonemura, S. Tsukita, and S. Tsukita. 1994. Perturbation of cell adhesion and microvilli formation by antisense oligonucleotides to ERM family members. *J. Cell Biol.* 125:1371–1384.

Taub, D.D., S.M. Turcovski-Corrales, M.L. Key, D.L. Longo, and W.J. Murphy. 1996. Chemokines and T lymphocyte activation: I. Beta chemokines costimulate human T lymphocyte activation in vitro. *J. Immunol.* 156:2095–2103.

Thuillier, L., C. Hivroz, R. Fagard, C. Andreoli, and P. Mangeat. 1994. Ligation of CD4 surface antigen induces rapid tyrosine phosphorylation of the cytoskeletal protein ezrin. *Cell. Immunol.* 156:322–331.

Tsukita, S.A., Y. Hieda, and S.H. Tsukita. 1989. A new 82-kD barbed end-capping protein (radixin) localized in the cell-to-cell adherens junction: purification and characterization. *J. Cell Biol.* 108:2369–2382.

Tsukita, S., S. Tsukita, A. Nagafuchi, and S. Yonemura. 1992. Molecular linkage between cadherins and actin filaments in cell-cell adherens junctions. *Curr. Opin. Cell Biol.* 4:834–839.

Tsukita, S., K. Oishi, N. Sato, J. Sagara, A. Kawai, and S. Tsukita. 1994. ERM family members as molecular linkers between the cell surface glycoprotein CD44 and actin-based cytoskeleton. *J. Cell Biol.* 126:391–401.

Tsukita, S., S. Yonemura, and S. Tsukita. 1997. ERM (ezrin/radixin/moesin) family: from cytoskeleton to signal transduction. *Curr. Opin. Cell Biol.* 9:70–75.

Wilkinson, P.C., and F.Y. Liew. 1995. Chemoattraction of human blood T lymphocytes by interleukin-15. *J. Exp. Med.* 181:1255–1259.

Winkler, B., C.G. Agostí, M. Magendantz, and F. Solomon. 1994. Analysis of a cortical cytoskeletal structure: a role for ezrin-radixin-moesin (ERM proteins) in the marginal band of chicken erythrocytes. *J. Cell Sci.* 107:2523–2534.

Yonemura, S., A. Nagafuchi, N. Sato, and S. Tsukita. 1993. Concentration of an integral membrane protein, CD43 (leukosialin, sialophorin), in the cleavage furrow through the interaction of its cytoplasmic domain with actin-based cytoskeleton. *J. Cell Biol.* 120:437–449.